Article

Not peer-reviewed version

Identification and Fine Mapping of Osdsm3, a Drought-Sensitive Gene in Rice (Oryza sativa L.)

Chenwei Deng , Yingxin Zhang , Beifang Wang , Hong Wang , Pao Xue , Yongrun Cao , Lianping Sun , Shihua Cheng , Liyong Cao * , Daibo Chen *

Posted Date: 2 August 2023

doi: 10.20944/preprints202308.0181.v1

Keywords: rice (Oryza sativa L.); Drought stress; Osdsm3; Genetic analysis; Fine mapping

Article

Identification and Fine Mapping of Osdsm3, a Drought-Sensitive Gene in Rice (*Oryza sativa* L.)

Chenwei Deng [1], Yingxin Zhang [1], Beifang Wang [1], Hong Wang [1], Pao Xue [1], Yongrun Cao [1], Lianping Sun [1], Shihua Cheng [1], Liyong Cao [1,2,*] and Daibo Chen [1,*]

[1] Key Laboratory for Zhejiang Super Rice Research, Chinese National Center for Rice Improvement and Stat Key Laboratory of Rice Biology, China National Rice Research Institute, Hangzhou 311401, China

[2] Baoqing Northern Rice Research Center, Northern Rice Research Center of China National Rice Research Institute, Baoqing 155600, China

* Correspondence: caoliyong@caas.cn (L.C.); cdb840925@163.com (D.C.); Tel.: +86-571-6337-0329 (L.C.); +86-571-6337-0606 (D.C.)

Abstract: Drought poses a significant constraint on rice production, and in this study, we have discovered a novel drought-sensitive mutant, designated as *dsm3*, arising from the progenies of indica rice variety Zhonghui8015 treated with EMS. Under drought stress conditions, *dsm3* exhibited characteristic withered leaf tips, accompanied by increased levels of MDA and H_2O_2, reduced Pn, and decreased activity of POD and SOD. Genetic analysis revealed that the withered leaf tip phenotype was governed by a single recessive gene, designated as *Osdsm3*.To begin with, *Osdsm3* was initially mapped to the short arm of chromosome 1 through a cross involving *dsm3* and 02428. Subsequently, utilizing a population of 2591 F2 individuals, we narrowed down the location of *Osdsm3* to a 78Kb interval, encompassing 13 open reading frames (ORFs). Sequencing analysis unveiled a mutation (1275G→A) in the exon of the candidate gene (LOC_Os01g10680), leading to premature translation termination. Moreover, a quantitative RT-PCR assay demonstrated high expression of *OsDSM3* in the panicle and sheath, with a significant upregulation of drought stress-related genes under drought conditions. Phylogenetic analyses indicated that *Osdsm3* shares evolutionary homology with UNE1, an intracellular transport protein found in Arabidopsis thaliana. Subcellular studies further confirmed that *OsDSM3* resides in the cytoplasm. In conclusion, the forthcoming cloning of *Osdsm3* holds promise for delving deeper into the molecular mechanisms governing rice drought resistance.

Keywords: rice (*Oryza sativa* L.); drought stress; *Osdsm3*; genetic analysis; fine mapping

1. Introduction

Rice (*Oryza sativa* L.) is a crucial crop that sustains more than half of the global population. However, drought stress stands as a prominent abiotic factor hindering rice yield, especially with the challenges of global warming and water scarcity [1]. Drought stress disrupts the delicate balance between water and carbon metabolism in rice, leading to osmotic disorders, reduced photosynthetic rates, and ultimately, diminished rice yields [2]. Identifying drought-tolerant genes is of paramount importance for both rice breeding and comprehensive molecular mechanism investigations.

Drought tolerance in rice primarily involves adaptive changes in root structure, osmotic adjustment, and antioxidant enzyme activities [3]. Under drought stress, rice experiences alterations in root architecture, including enhanced root-shoot ratios, increased fence-sponge tissue ratio, and thicker cuticles. These changes collectively minimize water loss, thus enhancing drought resistance [4,5]. As drought stress progresses, the number of nodal roots decreases, while lateral root branching density increases, along with elongation of total lateral root length [6,7]. Additionally, rice plants maintain cell osmolarity balance through osmotic adjustment substances like glycine betaine, trehalose, and soluble sugars during drought conditions [8]. Drought stress diminishes the activity of antioxidant enzymes such as superoxide dismutase (SOD), peroxidase (POD), and catalase (CAT),

 doi:10.20944/preprints202308.0181.v1

leading to the accumulation of reactive oxygen species (ROS) and resulting in cell metabolic disorders [9]. To mitigate the toxicity of excessive ROS, plants employ antioxidant enzymes like SOD and POD to scavenge the reactive oxygen species during drought stress [10].

Drought is a critical factor that hinders plant growth, impacting various stages of rice development and affecting both yield and quality [11]. To address production losses caused by drought stress, identifying drought-resistant genes and cultivating resilient rice varieties prove effective. Currently, researchers have isolated 44 drought-tolerant genes related to rice, categorized primarily into functional genes [12] and regulatory genes [13]. These genes participate in osmotic regulation, dehydration resistance, and antioxidant protection during drought stress [14]. For instance, Wei et al. identified and cloned a rice CDPK gene, *OsCPK9*, which enhances drought tolerance by improving osmotic regulation and enhancing stomatal closure. Ahmad et al. discovered the *OsTPKb* gene, a dual-pore potassium channel protein that maintains a normal K+ balance inside cells, thereby enhancing drought tolerance [15]. The *OsNHX1* (Na+/H+ Antiporter 1) gene plays a crucial role in ion balance regulation, affecting the concentration of intracellular sodium ions and increasing rice's drought tolerance, as found by Liu et al. Dehydration, a morphological response to drought stress, involves the waxy layer on the plant surface limiting transpiration rate, contributing to enhanced drought resistance [16]. Wang et al. discovered the *WSL4* gene, a β-ketoacyl-CoA synthase gene involved in rice leaf cuticular wax synthesis. Overexpression of this gene increases leaf cuticular wax content, reducing water loss, and enhancing drought resistance [17]. Additionally, under drought stress, plants accumulate reactive oxygen species (ROS) that can damage cellular structures and cause injuries. Antioxidant enzymes play a vital role in clearing ROS and mitigating plant damage. Du et al. observed that the expression levels of the peroxidase genes *OsPOX8.1* and *OsPOX22.3* increase during drought stress [18]. In a related study, Zhang et al. identified the gene *OsAPX2*, which encodes a cell solute ascorbate peroxidase. Overexpression of this gene significantly reduces ROS levels and positively regulates rice's drought tolerance [19]. Abcisic acid (ABA), a crucial hormone in plant responses to abiotic stress, also plays a vital role in drought response and regulation. Yu et al. discovered a drought-responsive gene called *OsEm1*, which enhances rice's sensitivity to ABA, positively regulating drought resistance [20]. Sharma et al. discovered the *OsFBX257* gene, a gene that encodes for an F-Box protein, which plays a crucial role in promoting ABA signaling. They observed that the gene's function and expression level have a significant impact on both root and shoot development, and it can also influence rice drought stress tolerance in controlled environments [21]. *OsbZIP23* and *OsbZIP72* are considered key regulators in ABA-dependent drought and salt stress responses. They control the expression of many stress-related genes and increase both ABA sensitivity and drought and salt resistance in rice [12,22,23]. Additionally, key enzyme genes involved in ABA biosynthesis and metabolism, such as *OsLCY* and *OsNCED4*, respond to rice drought stress by controlling the synthesis of ABA precursors [24,25]. Additionally, the NAC transcription factors in rice are significant players in responding to abiotic stress, with several NAC members involved in the response to drought stress. For instance, Hu et al. demonstrated that overexpressing the stress-responsive gene *SNAC1* significantly enhances drought resistance in transgenic rice, even under severe drought conditions during the reproductive phase, without affecting yield [26]. Moreover, PP2C protein phosphatases in plants have broad involvement in growth, development, and responses to biotic and abiotic stress, including disease resistance, wound response, and ABA-mediated stress signaling [27]. The OsPP2C gene family plays a crucial role in rice's response to drought stress, with *OsPP2C77*, *OsPP2C51*, and *OsPP2C49* confirmed to be involved in drought stress signal transduction. These discoveries shed light on the intricate mechanisms that contribute to rice's ability to cope with drought stress [28–30]. Overall, comprehending the functions of these drought-resistant genes and their regulatory mechanisms offers valuable insights to bolster rice's capacity to withstand drought stress, leading to enhanced crop yields and quality.

However, the current pool of cloned genes related to drought resistance in rice remains limited, hindering in-depth exploration of the molecular mechanisms involved. In this study, we conducted screening and characterization of a drought-sensitive mutant, followed by precise mapping to

 doi:10.20944/preprints202308.0181.v1

identify the candidate gene. Our findings contribute to a novel gene resource for breeding programs and facilitate investigations into the molecular mechanisms underlying drought resilience in rice.

2. Materials and Methods

2.1. Plant Materials

The drought-sensitive mutant (*dsm3*) was screened and identified from the mutant library of the indica rice cultivar Zhonghui8015 (ZH8015) treated with EMS (ethyl methanesulfonate). To conduct genetic analysis and gene mapping, a total of 2591 F2 individuals were generated through a cross between *dsm3* and 02428, a japonica rice cultivar. From 2017 to 2019, all plants were cultivated in an experimental field at the China National Rice Research Institute (Hangzhou, Zhejiang province, China) with a row spacing of 16.5 cm × 21.5 cm.

2.2. Measurement of agronomic traits

Both ZH8015 and *dsm3* plants were grown as described above. At the maturation stage, ten plants from the middle of each line were randomly selected for measuring agronomic traits. The measured traits included plant height, panicle length, grain length and width, thousand-grain weight, leaf length, and leaf width.

2.3. Drought stress treatments

To assess the drought tolerance of ZH8015 and *dsm3*, we conducted a modified drought stress treatment in the greenhouse of the China National Rice Research Institute in 2019 [31]. Germinated seeds were sown on a petri dish, and 7-day-old seedlings were then transplanted into plastic pots filled with 3 kg of sandy soil, which was irrigated daily. Subsequently, 7-week-old seedlings of ZH8015 and *dsm3* were subjected to varying durations of drought stress, including 0 days (Control Check, CK), 1, 2, 3, 4, 5, and 6 days. After the treatments, we collected samples of the second upper leaves, root system, and aboveground parts of all materials for determining physiological indices and conducting phenotype analysis. Additionally, soil water content was measured using the weighing method reported in the literature [32].

2.4. Histochemical and physiological analysis

To detect ROS accumulation, we followed previously reported methods [33]. For cell death detection, we detached the second upper leaves from the plants and stained them with a 1 mg/mL solution of 3,3'-diaminobenzidine (DAB) and a 0.25% solution of Evans blue (EB). After staining, the leaves were incubated with 95% ethanol at 85-90°C until chlorophyll was completely removed [34]. To determine cell size, we immersed 1 cm root-tips of ZH8015 and *dsm3* in a solution containing 1 μL of NerveRed and 1 mL of sterile water, allowing them to stand for 0.5 hours on ice under dark conditions. We followed the manufacturing instructions of NerveRed C2 (Item No: N4073) and captured images using a laser confocal scanning microscope (Zeiss LSM700, Germany). The net photosynthetic rate (Pn) of the second upper leaves of ZH8015 and *dsm3* was determined using a portable photosynthesis measurement device, LI-6400 (Li-COR, Lincoln, NB, USA), with an intensity of 1200 μmol protons (m2·s) and an airflow rate of 500 μmol·s-1 under drought stress. Chlorophyll was extracted from the second upper leaf tissues and determined by spectrophotometry as described previously [13]. Additionally, we determined the activity of SOD and POD, as well as the content of MDA, H_2O_2, soluble sugar, total protein, and proline using commercial assay kits from Nanjing Jiancheng Bioengineering Research Institute (China).

2.5. Primer Design and Sequencing

Genomic DNA was extracted from the leaves of recessive individuals using the CTAB method as previously described [35]. New SSR and InDel markers were designed using Primer Premier 5.0 software. The PCR reactions were performed using 2×Taq PCR Mix from TsingKe technology

 doi:10.20944/preprints202308.0181.v1

company (Hangzhou, China), and the PCR products were visualized on an 8.0% non-denaturing polyacrylamide gel. The primers used for PCR are listed in Table S1.

2.6. RNA extraction and qRT-PCR

Total RNAs were extracted using the RNAprep Pure Plant Kit (TIANGEN, Beijing), following the manufacturer's instructions. cDNA was synthesized using ReverTra Ace qPCR-RT Master Mix (Toyobo, Japan). qRT-PCR was performed using SYBR premix Ex Taq Ⅱ (Takala, Japan) on the LightCycler 480 Ⅱ (Roche, Sweden). UBQ was used as a reference gene. qRT-PCR was conducted to measure the expression levels of eight genes related to drought stress, including *OsbZIP23* [12], *OsbZIP72* [22], *POX22.3*, and *POX8.1* [36], *OsLCY* [24], *OsNCED4* [25], *OsPP2C* [28], and *OsSNAC1* [26]. The cycle threshold (Ct) 2–ΔΔCt method was used to analyze the relative gene expression. The primers used for qRT-PCR are listed in Table S2.

2.7. Sequence analysis

The open reading frame (ORFs) and full-length nucleotide sequences of *Osdsm3* were subjected to analysis using bioinformatics tools available on the websites RGAP (http://rice.plantbiology.msu.edu/) and NCBI (https://www.ncbi.nlm.nih.gov/). Nucleotide and amino acid sequence alignments were performed using MEGALIGN version 6 and SEQMAN version 6. Additionally, a phylogenetic tree was constructed using the neighbor-joining method with MEGA version 7.

2.8. Subcellular localization

The CDS of *Osdsm3* was cloned into the pYBA-1132-GFP vector without a termination codon, creating a fusion vector between *Osdsm3* and GFP. The fusion construct 35S::DSM3-GFP and a control vector 35S::GFP were introduced into rice protoplasts using the 40% PEG 6000-mediated method and incubated at 28°C for 24 hours under dark conditions. Confocal imaging was captured using a confocal laser scanning microscope (Zeiss LSM 700, Germany).

2.9. Statistical analysis

Statistical significance analysis was conducted using one-way analysis of variance. All trials were performed in three independent biological replicates and three technical replicates. The significant differences among various treatments are denoted by "*" at $p < 0.05$ and "**" at $p < 0.01$. Error bars represent the means ± SD ($n = 3$).

3. Results

3.1. Characterization of the dsm3 Mutant

Under drought stress, the *dsm3* mutant displayed a gradual withering of the leaf-tip at the tillering stage, starting 60 days after sowing (Figure 1A). Subsequently, the withered proportion extended along the leaf vein from the distal axis end to the proximal axis (Figure 1B). At the heading and maturation stages, the withering became more severe (Figure 1C,D). The appearance of the withered leaf-tip phenotype constrained the growth and development of *dsm3*, leading to reduced agronomic traits, including a decrease in thousand-grain weight and panicle length (Figure 1E, Table 1). Additionally, there were significant reductions in plant height, grain width, grain length-width ratio, flag leaf length, second upper leaf width, and third upper leaf width in *dsm3* compared to ZH8015 at the mature stage. However, there were no significant differences in the number of effective tillering (Table 1). These findings suggest that the withered leaf-tip in *dsm3* has a negative impact on its growth, development, and rice yield.

Preprints (www.preprints.org) | NOT PEER-REVIEWED | Posted: 2 August 2023 doi:10.20944/preprints202308.0181.v1

Figure 1. Phenotype of *dsm3* mutant under drought stress. (**A**,**B**): Plant architecture and leaf tip phenotype of ZH8015 and *dsm3* at sowing 60 days under drought stress, respectively. (**C**,**D**): The plant height of *dsm3* significantly decreased at the heading and maturation stage. (**E–G**): comparison of panicle length, grain width and length between ZH8015 and *dsm3* at the maturation stage, respectively. (**A**,**B**) scale bar=10 cm. (**D**,**E**) scale bar=2 cm. (**F**,**G**) scale bar=1 cm.

Table 1. Comparison with agronomic traits between ZH8015 and *dsm3* under drought stress.

Trait	ZH8015	*dsm3*
Plant height (cm)	101.90 ± 2.70	71.25 ± 3.16 **
No.of effective tillerings	6.30 ± 1.80	6.70 ± 1.40
Grain length (cm)	1.01 ± 0.10	0.97 ± 0.13 *
Grain width (cm)	0.33 ± 0.04	0.29 ± 0.05 *
Grain length-width ratio	0.31 ± 0.05	0.33 ± 0.07 **
Thousand grain weight (g)	38.33 ± 0.99	26.91 ± 1.53 **
Panicle length (cm)	24.40 ± 1.40	18.80 ± 1.14 **
Flag leaf length (cm)	30.38 ± 4.11	22.33 ± 3.11 **
Flag leaf width (cm)	1.58 ± 0.09	1.26 ± 0.13 *
Second upper leaf length (cm)	41.66 ± 4.64	33.87 ± 4.00 *
Second upper leaf width (cm)	1.48 ± 0.12	1.25 ± 0.07 **
Third upper leaf length (cm)	45.68 ± 4.60	41.33 ± 3.59 *
Third upper leaf width (cm)	1.52 ± 0.12	1.25 ± 0.08 **

* $p < 0.05$ compared with ZH8015, ** $p < 0.01$ compared with ZH8015.

3.2. Sensitivity of dsm3 to Drought Stress

To assess the response to drought stress, ZH8015 and *dsm3* plants were subjected to irrigation cessation from 0 to 6 days after sowing at day 46. The withered leaf-tip phenotype of *dsm3* emerged after 2 days of treatment and worsened with prolonged exposure, while ZH8015 did not exhibit such symptoms (Figure 2A). During the treatment period from 0 to 4 days, both ZH8015 and *dsm3* experienced gradual reductions in maximum root length and root-shoot ratio (Figure 2B,C,E). Notably, *dsm3* displayed a significant decrease in maximum root length after 2 days of treatment (Figure 2C). Despite the similar decline in soil relative moisture content in both ZH8015 and *dsm3*

Preprints (www.preprints.org) | NOT PEER-REVIEWED | Posted: 2 August 2023 doi:10.20944/preprints202308.0181.v1

(Figure 2D), the inhibited root growth in *dsm3* suggested its sensitivity to dehydration stress. Furthermore, the significant reduction in soil relative moisture of ZH8015 after 4 days of treatment indirectly indicated a decrease in the root water use efficiency of *dsm3* (Figure 2E). We speculate that differences in root water use efficiency between ZH8015 and *dsm3* contributed to the significant decrease in maximum root length and root-shoot ratio observed in *dsm3*.Additionally, this study examined the activities of SOD and POD, as well as the content of total protein and MDA. The results revealed that ZH8015 showed stronger activities of POD and SOD and higher total protein content compared to the *dsm3* mutant under drought stress (Figure 2G,I). Conversely, there was a significant decrease in the MDA content of *dsm3* compared to ZH8015 (Figure 2H). The changes in phenotypic and physiological indicators indicated the sensitivity of *dsm3* to drought stress.

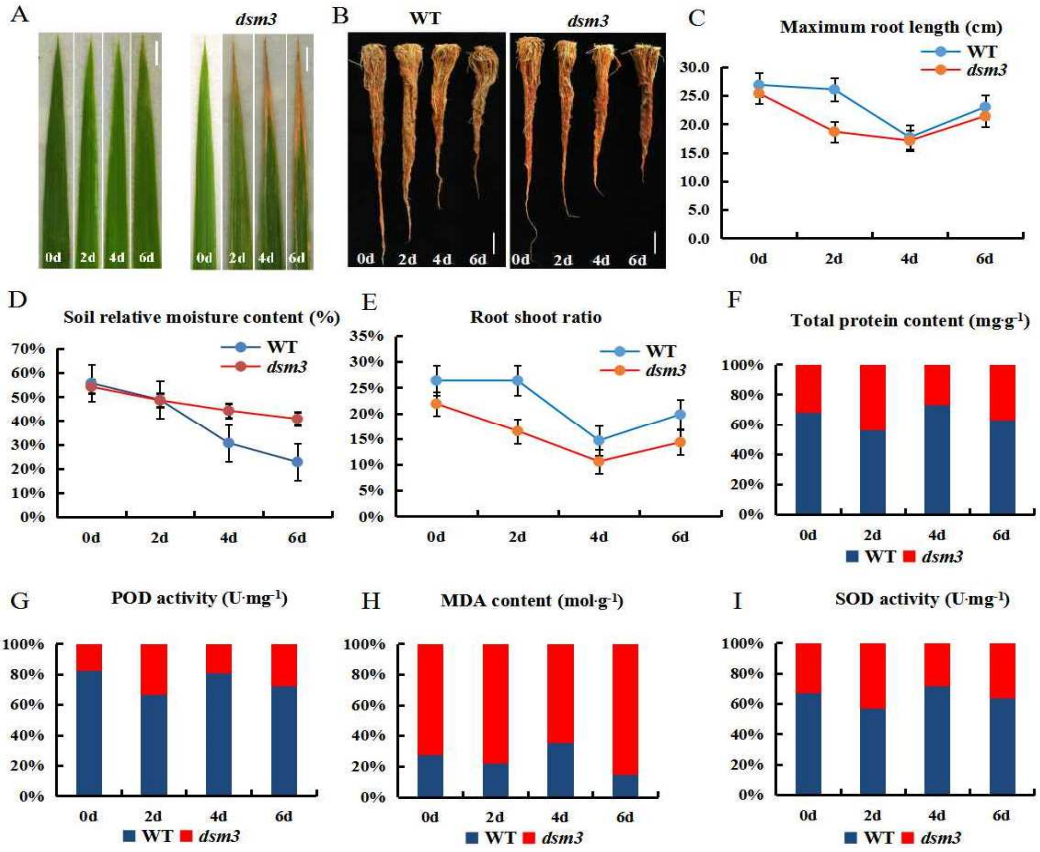

Figure 2. Response to drought treatment of ZH8015 and *dsm3* at the tillering stage. (**A**): The leaves tip phenotype comparison of ZH8015 and *dsm3* after stress treatment of 2d, 4d, and 6d. (**B**,**C**): The Maximum root length of ZH8015 and *dsm3* exhibited variation trend as the stress treatment time prolonged. (**D**): The Chart of root-shoot ratio variation tendency between ZH8015 and *dsm3* under drought stress. (**E**): Soil relative moisture of ZH8015 and *dsm3* decreased gradually with the extension of stress treatment time. F-I: Statistical analysis of total protein content (**F**), POD activity (**G**), MDA content (**H**), and SOD activity (**I**) in ZH8015 and *dsm3* after drought stress. (**A**) scale bar=10 cm. (**B**) scale bar=2 cm (n=3).

3.3. Abnormal H_2O_2 Accumulation, Cell Death, and Altered Cell Size in the Root Apical Meristem of the dsm3 Mutant

We hypothesized that the withered leaf-tip of *dsm3* resulted from an accumulation of H_2O_2 leading to cell death. Evans blue staining revealed numerous blue spots in *dsm3* after staining, indicating a significant accumulation of dead cells compared to ZH8015 (Figure 3A). Additionally, DAB staining demonstrated a much stronger H_2O_2 accumulation in *dsm3* leaves compared to ZH8015 after staining (Figure 3B). To assess cell size, we treated the root-tips of ZH8015 and *dsm3* with NerveRed, a fluorescent dye, and examined them using a laser confocal scanning microscope (Figure

Preprints (www.preprints.org) | NOT PEER-REVIEWED | Posted: 2 August 2023 doi:10.20944/preprints202308.0181.v1

3C). The results revealed that the root apical meristem cells of ZH8015 and *dsm3* were closely arranged, while the root apical meristem cells of *dsm3* appeared narrower and shorter. This finding explains why ZH8015 exhibited a longer maximum root length compared to *dsm3*.

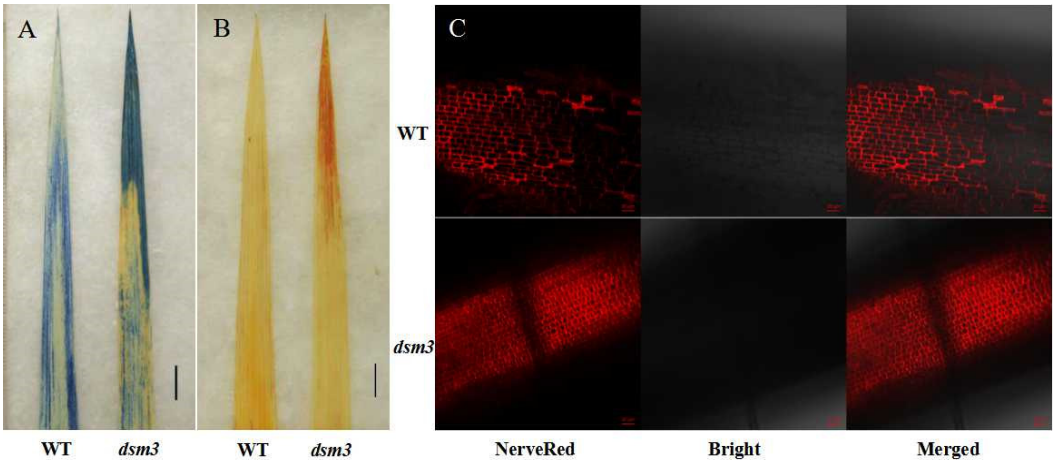

Figure 3. Histochemical staining of ZH8015 and *dsm3* to assay the presence of H_2O_2 , dead cell and cell size. (**A**): Leaf Evans blue staining of ZH8015 and *dsm3* to assay the presence of dead cells. (**B**): Leaf DAB staining of ZH8015 and *dsm3* to monitor the presence of H_2O_2. (**C**): NerveRed staining assay carried out to measure the cell size in root apical meristem between ZH8015 and *dsm3*. (**A**,**B**) scale bar=1 cm. (**C**) scale bar=20 um.

3.4. Evaluation of Photosynthetic and Physiological Indicators under Drought Stress

Drought stress disrupts the carbon metabolism balance in plant cells, negatively affecting photosynthesis. To assess this, we measured the photosynthetic pigment content and net photosynthetic rate (Pn). Under drought stress, *dsm3* leaves exhibited a significant reduction in Chla content and Pn compared to ZH8015 (Figure 4A,B). Furthermore, there was a notable decrease in stomatal conductance and intercellular CO_2 concentration in *dsm3* leaves (Figure 4C). Next, we measured various indicators in ZH8015 and *dsm3* at the tillering stage under drought stress, including total protein, proline, MDA, H_2O_2, soluble sugar, and the activities of SOD and POD. The results indicated substantially higher levels of proline, MDA, and H_2O_2 in DSM3 compared to ZH8015 (Figure 4F,G,H), while *dsm3* exhibited lower total protein content than ZH8015 (Figure 4E). Additionally, the soluble sugar content and POD activity were significantly decreased in *dsm3* compared to ZH8015, and SOD activity was also notably reduced (Figure 4I,J,K). Based on these findings, we postulate that the reduced activities of SOD and POD in *dsm3* may hinder the scavenging of oxidative metabolites, leading to the disruption of cell membrane integrity, cell death, and a weakened drought tolerance.

Preprints (www.preprints.org) | NOT PEER-REVIEWED | Posted: 2 August 2023 doi:10.20944/preprints202308.0181.v1

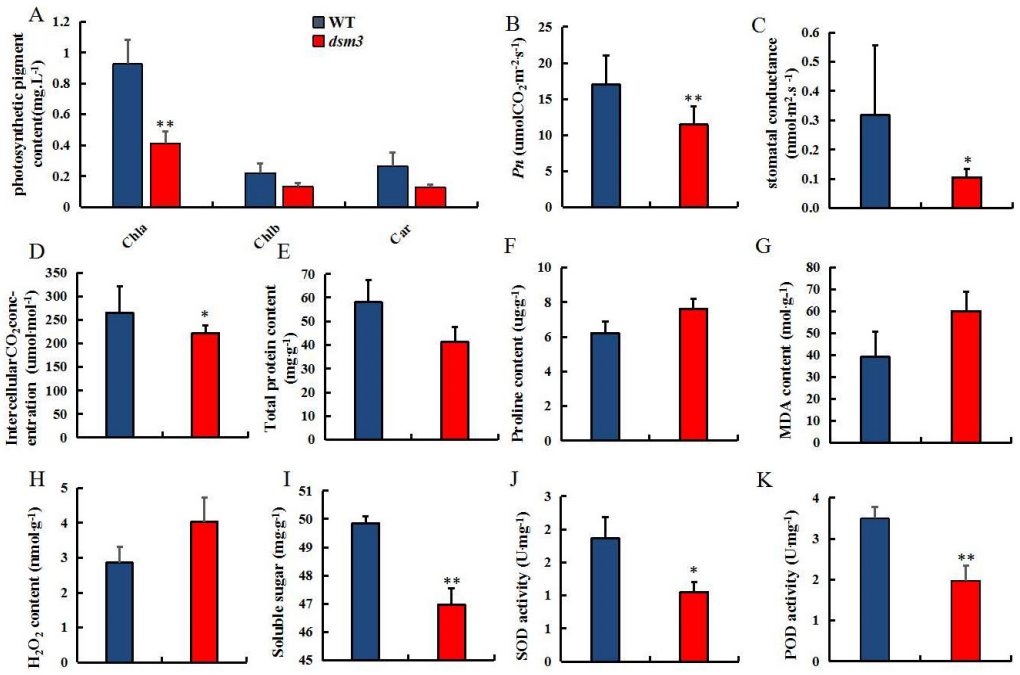

Figure 4. Measurement of drought related physiological traits in ZH8015 and *dsm3* under drought stress. (**A**): The levels of Chla, Chlb, and Car measured in ZH8015 and *dsm3* after drought stress. (**B**–**D**): Statistical analysis of the Pn, stomatal conductance, and intercellular CO_2 concentration in ZH8015 and *dsm3* at the tillering stage after drought stress. (**E**–**K**): Statistical analysis of total protein content (**E**), proline content (**F**), MDA content (**G**), H_2O_2 content (**H**), Soluble sugar content (**I**), SOD activity (**J**), and POD activity (**K**) in ZH8015 and *dsm3* at the tillering stage after drought stress. (Mean ±SD, n=3).

3.5. Genetic Analysis and Fine Mapping of Osdsm3

In the F_1 generation resulting from the cross between *dsm3* and 02428, all individuals exhibited a normal phenotype. The segregation ratios in the F2 population followed a 3:1 pattern, with χ^2=2.64 $<\chi^2_{0.05}$=3.84 (Table 2), indicating that the phenotype of *dsm3* was governed by a single recessive gene.

To identify the *Osdsm3* locus, the recessive mutant plants from the F2 population were subjected to map-based cloning. Linkage analysis revealed that the *Osdsm3* locus was linked to the RM3746 marker on chromosome 1. Subsequently, newly developed SSR markers and InDel markers were employed to analyze 37 recessive mutant plants, which initially mapped the *Osdsm3* locus to a 7.78 Mb interval between RM8068 and C102 on the short arm of chromosome 1 (Figure 5A). With the inclusion of 749 recessive individuals, the *Osdsm3* locus was further narrowed down to a 78 Kb interval between the C272 and RM223 markers (Figure 5B). Within this region, a total of 13 open reading frames (ORF) were identified based on the Rice Genome Annotation Project (http://rice.plantbiology.msu.edu/). PCR amplification of the CDS and genome sequences of these 13 ORFs was performed. The sequencing results indicated a mutation of 1275G→A in the exon of ORF6 (LOC_Os01g10680), resulting in TGG→TGA, leading to premature translation termination (Figure 5C). LOC_Os01g10680 encodes a putative protein known as GIL1 (gravitropic in the light), consisting of 520 amino acids with a molecular mass of 56.48kD. This protein belongs to the plant protein family DUF641, whose function is currently not well understood. Meanwhile, no mutations were found in the other 12 candidate genes between ZH8015 and *dsm3*. Therefore, LOC_Os01g10680 was identified as the target gene.

Preprints (www.preprints.org) | NOT PEER-REVIEWED | Posted: 2 August 2023 doi:10.20944/preprints202308.0181.v1

Table 2. Genetic analysis of *dsm3* in F_2 population.

F_2 population	F_1 generation	N0. of normal plants	No. of mutant plants	Theoretic ratio	Chi-square value
dsm3×02428	Normal	2591	809	3:1	2.64

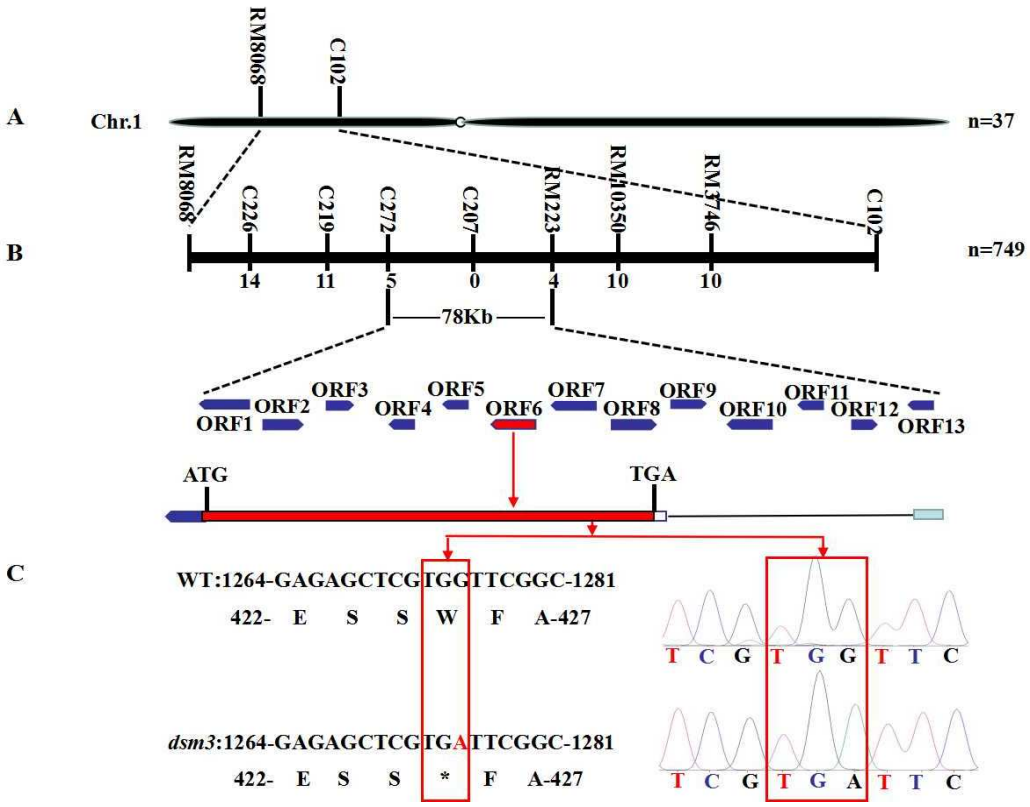

Figure 5. Fine mapping of *Osdsm3*. (**A**): Primary mapping of *Osdsm3* locus. The character above the chromosome represented the SSR and IeDel markers. And the number on the right side of chromosome indicated the recessive mutant, as the same below. (**B**): Fine mapping of *Osdsm3* locus. Numbers under the chromosome indicated the No. of recombinants. The 13 ORFs in the 78 Kb interval represented the blue rectangle. (**C**): The *Osdsm3* gene structure. The *Osdsm3* gene containing one exon and one intron indicated by using the red-rectangle and black line, respectively, a mutation from G to A in the exon caused premature translation termination.

3.6. Analysis of Osdsm3 Expression Levels and Drought Stress-Related Genes

To investigate the regulatory role of *Osdsm3* in the drought stress mechanism, we conducted qRT-PCR analysis to measure the expression levels of two ROS-scavenging enzymes (*OsPOX22.3*, *OsPOX8.1*), two genes related to ABA synthesis (*OsLCY*, *OsNCED4*), and four genes associated with drought tolerance (*OsbZIP23*, *OsbZIP72*, *OsNAC1*, *OsPP2X*) in both ZH8015 and *dsm3*. The results showed that the transcript levels of *OsbZIP23*, *OsPOX8.1*, and *OsNCED4* were significantly up-regulated in *dsm3* compared to ZH8015. In contrast, the transcript level of *OsLCY* was markedly down-regulated in *dsm3* when compared to ZH8015 (Figure 6A). Notably, the transcript levels of *OsNCED4* and *OsLCY* were upregulated by 5.1- and downregulated by 2.6-fold, respectively. Based on these findings, we speculate that the expression of genes related to drought resistance in *dsm3* is induced in response to drought stress, and the response of *dsm3* to drought stress may be regulated by ABA-dependent mechanisms.

Furthermore, the RT-PCR results indicated that the transcript level of *Osdsm3* was significantly higher in *dsm3* than in ZH8015 (Figure 6B). A tissue-specific expression analysis revealed that *OsDSM3* expression was highest in young panicles, approximately 1.44-fold in leaf sheaths, and around 3.96-

Preprints (www.preprints.org) | NOT PEER-REVIEWED | Posted: 2 August 2023 doi:10.20944/preprints202308.0181.v1

fold in roots (Figure 6C). These findings suggest that *Osdsm3* not only functions in drought tolerance but also plays a key role in grain yield formation, which is consistent with the results showing changes in grain size (Figure 1F–G).

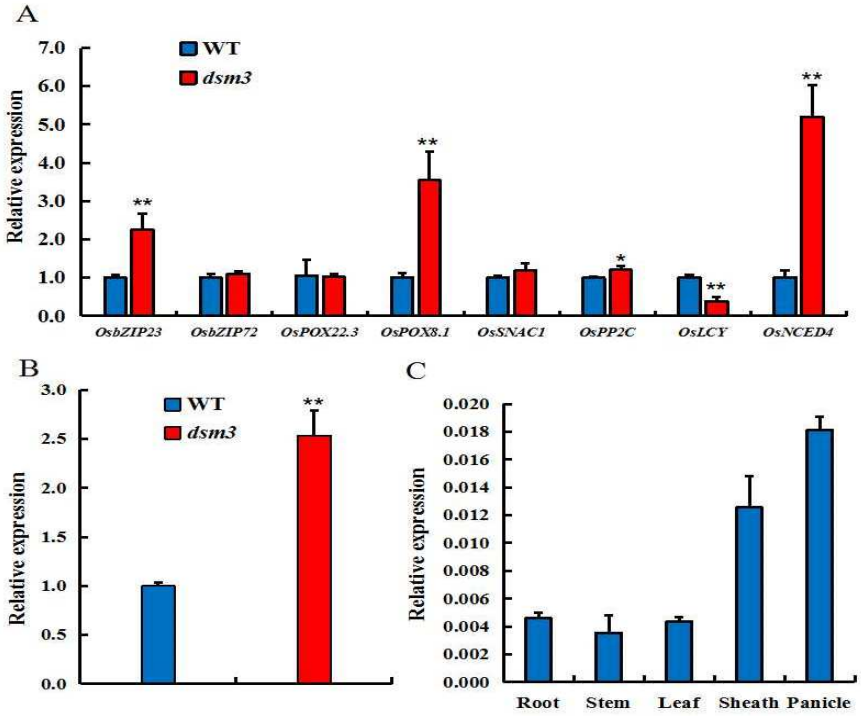

Figure 6. Expression level and pattern analysis of *Osdsm3* and dehydration stress-related genes in ZH8015 and *dsm3* under drought stress. (**A**): The relative expression levels of drought stress-associated genes were measured using qRT-PCR in ZH8015 and *dsm3* under drought stress. The transcript level expressed relative to a UBQ reference gene. (**B**): Relative expression level of *Osdsm3* in ZH8015 and *dsm3*. The relative expression level of *Osdsm3* in *dsm3* was normalized to that of ZH8015. (**C**): The tissue-specific expression of *Osdsm3* was analysed in ZH8015.

3.7. Phylogenetic Analysis and Subcellular Localization of OsDSM3

A phylogenetic tree of *Osdsm3* (LOC_Os01g10680) and other plant DUF641 family proteins was constructed using the neighbor-joining method with 1000 bootstrap replications via MEGA version 7 software. The phylogenetic analysis revealed that *Osdsm3* shared high homology with UNE1, an intracellular transporter protein (Accession: NP_174224) found in Arabidopsis thaliana (Figure 7A). According to information from TAIR (https://www.arabidopsis.org/), intracellular transport proteins not only respond to gravity, red light, and far-red light but also participate in the double fertilization process of plants.

To determine the subcellular localization of *OsDSM3*, a 35S:: DSM3-GFP fusion construct, and a control 35S:: GFP construct were created using the pYBA-1132-GFP vector, and then transferred into rice protoplasts using the PEG 6000-mediated method. After incubating the transformed rice protoplasts for 24 hours at indoor temperature, the green fluorescence signal was detected at 488 nm using a laser scanning microscope. The results showed that the 35S:: DSM3-GFP fluorescence signal was exclusively distributed in the cytoplasm, while the control 35S:: GFP fluorescence signal was observed throughout the cell (Figure 7B). These findings indicate that *OsDSM3* is a cytoplasm-localized protein.

Preprints (www.preprints.org) | NOT PEER-REVIEWED | Posted: 2 August 2023 doi:10.20944/preprints202308.0181.v1

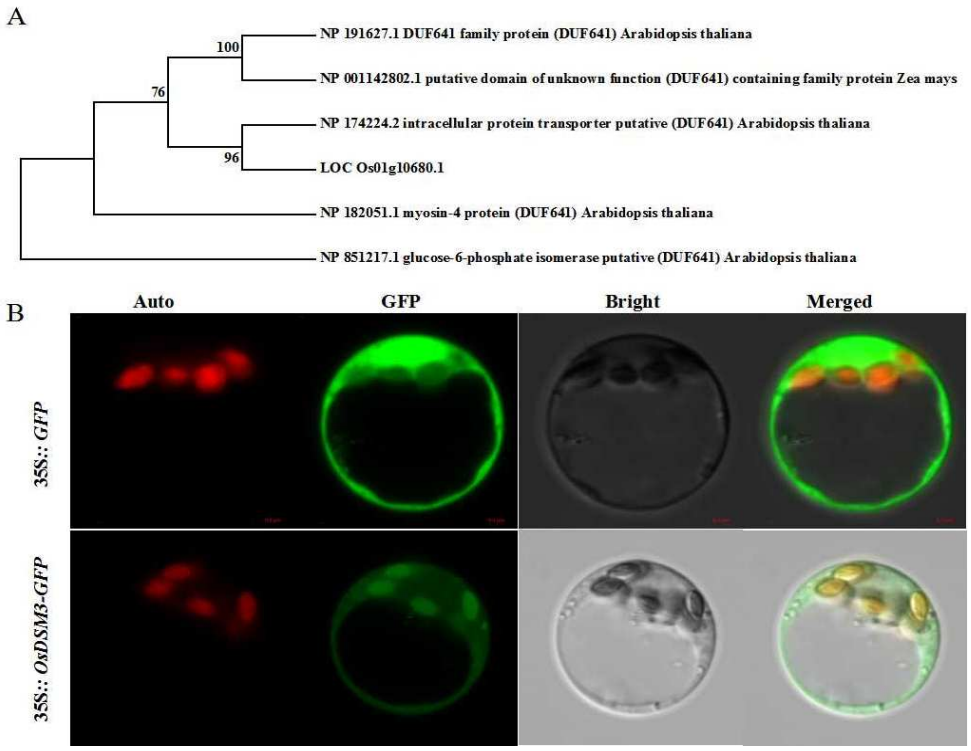

Figure 7. Phylogenetic analysis and Subcellular localization of *OsDSM3*. (**A**): The Phylogenetic relationship of DUF641 protein family among indica rice ZH8015, Arabidopsis thaliana and Zea mays determined using the neighbor-joining method with MEGA version 7 software. Genebank accession number for amino acid sequences: AT1G29300 (UNE1), AT3G60680, AT2G45260, AT5G58960, and ZEAMMB73_Zm00001d032503. (**B**): Subcellular localization of the *Osdsm3* protein in rice protoplasts. A fusion vector 35S:: DSM3-GFP and a control 35S:: GFP were transferred into rice protoplasts. The green fluorescence signal was detected at an excitation wavelength 488 nm using a laser scanning microscope. scale bars=2 um.

4. Discussion

Plants often face challenges from both biotic and abiotic factors, such as drought, salt, and cold stress, leading to physiological and biochemical changes at the cellular and molecular levels [37]. In previous studies, the dsm1 mutant showed drought sensitivity during the seeding and booting stages, while overexpression of the *DSM1* gene enhanced drought resistance in rice seedlings [36]. Similarly, the dsm2 mutant exhibited drought hypersensitivity during the seedling and panicle development stages, showing higher levels of wilting and MDA content compared to wild-type plants after dehydration stress [38]. In this study, we focused on the *dsm3* mutant, which displayed drought sensitivity during the tillering stage and showed a significant decrease in agronomic traits related to rice yield (Table 1). Furthermore, under drought stress, the content of MDA and H_2O_2 in *dsm3* was higher than that in WT plants (Figure 4G,H).

The reduction in total chlorophyll content and leaf area in *dsm3* might have contributed to the decrease in the net photosynthetic rate (Figure 4A,B). Drought stress disrupted the ROS homeostasis in plant cells, resulting in ROS accumulation and the breakdown of membrane lipids [39], which could cause cell death in *dsm3*, as confirmed by Evans blue staining (Figure 2A). The reduced stomatal conductance of *dms3* weakened its ability to absorb CO_2 from the environment, leading to a decrease in intercellular CO_2 concentration and insufficient fixation of CO_2 during the photosynthetic dark reaction phase. Consequently, dry matter accumulation was reduced, consistent with the change in thousand-grain weight (Table 1).These results indicate that *dms3* is a drought-sensitive mutant and exhibits unique responses under drought stress. Understanding the underlying mechanisms of its

 doi:10.20944/preprints202308.0181.v1

drought sensitivity may provide valuable insights into developing strategies for enhancing drought resistance in rice and other crops

Peroxidases are found universally in vascular plants and play a crucial role in defending against abiotic stress such as drought, salt, and heat by scavenging reactive oxygen species (ROS) [40]. In the case of the peroxidase gene *OsPOX8.1*, its expression level was higher in *dsm3* compared to ZH8015, but surprisingly, the peroxidase activity (POD) was significantly reduced in *dsm3* (Figure 6A). This led us to conclude that the POD expression might be activated due to the accumulation of peroxides. Further investigations, including peroxidase activity assays, superoxide dismutase tests, and DAB staining, revealed that *dsm3* suffered damage from ROS accumulation, which aligned with Jing's research [36].

Earlier studies have suggested that stress-related genes respond to drought stress through ABA-dependent or ABA-independent pathways [41,42]. In our study, we performed a comparative analysis of drought stress-related genes in *dsm3* and ZH8015 (Figure 6A). Notably, the gene *OsNCED4*, responsible for catalyzing the rate-limiting step of ABA biosynthesis, showed a significant increase in relative transcript levels under drought stress [24]. Simultaneously, the upstream gene *OsLCY*, responsible for ABA biosynthesis through carotene conversion, exhibited significant down-regulation under drought stress [25]. The varying expression levels of *OsNCED4* and *OsLCY* support their role in ABA biosynthesis, as previously described. Consequently, we speculated that the *dsm3* response to drought stress might be regulated through the ABA-dependent pathway. Additionally, we observed that *Osdsm3* exhibited the highest relative transcript abundance in young panicles, while the grain-weight of *dsm3* reduced significantly (Figure 6C, Table 1). This indicates that *Osdsm3* might be a multifunctional gene, playing a role in both rice yield and response to drought.

The candidate interval comprised 13 ORFs, of which ORFs 1 to 5 and 11 to 13 encoded proteins of unknown function, as described in RGAP (Table S1). Additionally, ORF7 encoded a δ-composite subunit involved in DNA polymorphism, consisting of a POLD1/p123 catalytic unit and three regulatory units—POLD2/p50, POLD3/p66, and POLD4/p12. This subunit played a crucial role in DNA repair mechanisms [43]. ORF8 encoded an immune protein with a domain containing collagen fiber and cyclic carbohydrates, facilitating the recognition of specific microbial surface carbohydrates and participating in immune responses to pathogen infections [44]. ORF9 encoded a receptor-like protein kinase, responsible for sensing and transducing stress signals, and regulating downstream gene expression through phosphorylation and dephosphorylation to combat biotic and abiotic stresses [45]. Notably, all of these genes exhibited identical sequences between ZH8015 and *dsm3*.

Moving on to ORF6, it encoded a GIL1 protein, which in Arabidopsis thaliana was induced simultaneously by light and gravity. In experiments with the loss-of-function gil1 mutant exposed to red light and far-red light in the presence of gravity, its hypocotyl growth occurred in the anti-gravity direction. However, there were no phenotype changes when it was solely induced by gravity or light [46]. Nonetheless, further investigation is needed to determine whether ORF6 influences the growth direction of rice hypocotyls. No insertions, deletions, transitions, or transversions were found in the other ORFs, except for a single base mutation in the exon of ORF6 (*Osdsm3*), leading to premature translation termination. Based on these findings, ORF6 was identified as the candidate gene. The identified mutation site, *Osdsm3*, which results in the formation of a premature stop codon, offers a compelling opportunity for gene editing to create relatively weaker mutant variants. This approach holds the potential to establish a harmonious balance between crop yield and drought resistance, enabling the identification of suitable loci that confer both improved drought tolerance and maintained productivity. By exploring and harnessing these beneficial mutation sites, novel resources for water-efficient and drought-resistant rice varieties can be developed, contributing significantly to the advancement of sustainable agriculture practices. However, its gene function requires verification through transgenic complementary experiments.

5. Conclusions

In this study, we conducted a screening and characterization of a drought-sensitive mutant, named *dsm3*, from the progenies of indica rice variety Zhonghui 8015 treated with EMS. Through

phenotypic analysis and drought stress evaluation, we established that *dsm3* exhibited sensitivity to drought stress. The underlying cause of the *dsm3* phenotype was traced back to the *Osdsm3* gene, which was located within a 78kb interval between markers C272 and RM223 on the short arm of chromosome 1. Initial insights into the function of *Osdsm3* were gained through phylogenetic analysis and subcellular localization studies. Subsequent map-based cloning of *Osdsm3* will further our understanding of the molecular mechanisms behind drought resistance in rice and pave the way for developing new drought-resistant rice cultivars.

Supplementary Materials: The following supporting information can be downloaded at the website of this paper posted on Preprints.org, Table S1: Candidate genes in target region; Table S2: Primers used for gene mapping, subcellular localization and RT-qPCR.

Author Contributions: Data curation, Chenwei Deng; Funding acquisition, Shihua Cheng and Liyong Cao; Investigation, Beifang Wang, Hong Wang, Pao Xue and Yongrun Cao; Methodology, Chenwei Deng; Resources, Yingxin Zhang; Supervision, Yingxin Zhang and Lianping Sun; Writing – original draft, Chenwei Deng; Writing – review & editing, Yingxin Zhang, Lianping Sun and Daibo Chen. All authors have read and agreed to the published version of the manuscript..

Funding: This research was funded by National Natural Science Foundation of China, grant number 31961143016; Fundamental Research Funds of Central Public Welfare Research Institutions, grant number CPSIBRF-CNRRI-202102; Chinese Academy of Agricultural Sciences Innovation Project, grant number ASTIP-2013-CNRRI; China Agriculture Research System, grant Number CARS-01-03; Zhejiang Provincial Key Special Projects, grant number 2021C02063-1.

Data Availability Statement: Not applicable.

Conflicts of Interest: The authors declare no conflict of interest.

References

1. Upadhyaya, H.; Panda, S.K. Drought stress responses and its management in rice. In *Advances in rice research for abiotic stress tolerance*; Elsevier: 2019; pp. 177-200.
2. Yang, X.; Wang, B.; Chen, L.; Li, P.; Cao, C. The different influences of drought stress at the flowering stage on rice physiological traits, grain yield, and quality. *Scientific reports* **2019**, *9*, 3742.
3. Kim, Y.; Chung, Y.S.; Lee, E.; Tripathi, P.; Heo, S.; Kim, K.H. Root Response to Drought Stress in Rice (Oryza sativa L.). *Int J Mol Sci* **2020**, *21*, doi:10.3390/ijms21041513.
4. Salsinha, Y.C.F.; Maryani; Indradewa, D.; Purwestri, Y.A.; Rachmawati, D. Leaf physiological and anatomical characters contribute to drought tolerance of Nusa Tenggara Timur local rice cultivars. *Journal of Crop Science and Biotechnology* **2021**, *24*, 337-348.
5. Xu, W.; Cui, K.; Xu, A.; Nie, L.; Huang, J.; Peng, S. Drought stress condition increases root to shoot ratio via alteration of carbohydrate partitioning and enzymatic activity in rice seedlings. *Acta physiologiae plantarum* **2015**, *37*, 1-11.
6. Hazman, M.; Brown, K.M. Progressive drought alters architectural and anatomical traits of rice roots. *Rice (N Y)* **2018**, *11*, 62, doi:10.1186/s12284-018-0252-z.
7. Ranjan, A.; Sinha, R.; Singla-Pareek, S.L.; Pareek, A.; Singh, A.K. Shaping the root system architecture in plants for adaptation to drought stress. *Physiol Plant* **2022**, *174*, e13651, doi:10.1111/ppl.13651.
8. Redillas, M.C.; Park, S.-H.; Lee, J.W.; Kim, Y.S.; Jeong, J.S.; Jung, H.; Bang, S.W.; Hahn, T.-R.; Kim, J.-K. Accumulation of trehalose increases soluble sugar contents in rice plants conferring tolerance to drought and salt stress. *Plant Biotechnology Reports* **2012**, *6*, 89-96.
9. Wang, X.; Liu, H.; Yu, F.; Hu, B.; Jia, Y.; Sha, H.; Zhao, H. Differential activity of the antioxidant defence system and alterations in the accumulation of osmolyte and reactive oxygen species under drought stress and recovery in rice (Oryza sativa L.) tillering. *Sci Rep* **2019**, *9*, 8543, doi:10.1038/s41598-019-44958-x.
10. Sales, C.R.; Ribeiro, R.V.; Silveira, J.A.; Machado, E.C.; Martins, M.O.; Lagoa, A.M. Superoxide dismutase and ascorbate peroxidase improve the recovery of photosynthesis in sugarcane plants subjected to water deficit and low substrate temperature. *Plant Physiol Biochem* **2013**, *73*, 326-336, doi:10.1016/j.plaphy.2013.10.012.

11. Oladosu, Y.; Rafii, M.Y.; Samuel, C.; Fatai, A.; Magaji, U.; Kareem, I.; Kamarudin, Z.S.; Muhammad, I.; Kolapo, K. Drought Resistance in Rice from Conventional to Molecular Breeding: A Review. *Int J Mol Sci* **2019**, *20*, doi:10.3390/ijms20143519.
12. Xiang, Y.; Tang, N.; Du, H.; Ye, H.; Xiong, L. Characterization of OsbZIP23 as a key player of the basic leucine zipper transcription factor family for conferring abscisic acid sensitivity and salinity and drought tolerance in rice. *Plant Physiol* **2008**, *148*, 1938-1952, doi:10.1104/pp.108.128199.
13. Zhang, L.; Kusaba, M.; Tanaka, A.; Sakamoto, W. Protection of Chloroplast Membranes by VIPP1 Rescues Aberrant Seedling Development in Arabidopsis nyc1 Mutant. *Front Plant Sci* **2016**, *7*, 533, doi:10.3389/fpls.2016.00533.
14. Aroca, R. Plant responses to drought stress. *From Morphological to Molecular Features; Springer: Berlin/Heidelberg, Germany* **2012**, 1-5.
15. Ahmad, I.; Devonshire, J.; Mohamed, R.; Schultze, M.; Maathuis, F.J. Overexpression of the potassium channel TPKb in small vacuoles confers osmotic and drought tolerance to rice. *New Phytol* **2016**, *209*, 1040-1048, doi:10.1111/nph.13708.
16. Liu, S.; Zheng, L.; Xue, Y.; Zhang, Q.; Wang, L.; Shou, H. Overexpression of OsVP1 and OsNHX1 increases tolerance to drought and salinity in rice. *Journal of Plant Biology* **2010**, *53*, 444-452.
17. Wang, X.; Guan, Y.; Zhang, D.; Dong, X.; Tian, L.; Qu, L.Q. A β-ketoacyl-CoA synthase is involved in rice leaf cuticular wax synthesis and requires a CER2-LIKE protein as a cofactor. *Plant Physiology* **2017**, *173*, 944-955.
18. Du, H.; Liu, L.; You, L.; Yang, M.; He, Y.; Li, X.; Xiong, L. Characterization of an inositol 1, 3, 4-trisphosphate 5/6-kinase gene that is essential for drought and salt stress responses in rice. *Plant molecular biology* **2011**, *77*, 547-563.
19. Zhang, Z.; Zhang, Q.; Wu, J.; Zheng, X.; Zheng, S.; Sun, X.; Qiu, Q.; Lu, T. Gene knockout study reveals that cytosolic ascorbate peroxidase 2 (OsAPX2) plays a critical role in growth and reproduction in rice under drought, salt and cold stresses. *PloS one* **2013**, *8*, e57472.
20. Yu, J.; Lai, Y.; Wu, X.; Wu, G.; Guo, C. Overexpression of OsEm1 encoding a group I LEA protein confers enhanced drought tolerance in rice. *Biochem Biophys Res Commun* **2016**, *478*, 703-709, doi:10.1016/j.bbrc.2016.08.010.
21. Sharma, E.; Bhatnagar, A.; Bhaskar, A.; Majee, S.M.; Kieffer, M.; Kepinski, S.; Khurana, P.; Khurana, J.P. Stress-induced F-Box protein-coding gene OsFBX257 modulates drought stress adaptations and ABA responses in rice. *Plant Cell Environ* **2023**, *46*, 1207-1231, doi:10.1111/pce.14496.
22. Lu, G.; Gao, C.; Zheng, X.; Han, B. Identification of OsbZIP72 as a positive regulator of ABA response and drought tolerance in rice. *Planta* **2009**, *229*, 605-615, doi:10.1007/s00425-008-0857-3.
23. Pa, V.; Vijayaraghavareddy, P.; Uttarkar, A.; Dawane, A.; D, S.; V, A.; Kc, B.; Niranjan, V.; Ms, S.; Cv, A.; et al. Novel small molecules targeting bZIP23 TF improve stomatal conductance and photosynthesis under mild drought stress by regulating ABA. *FEBS J* **2022**, *289*, 6058-6077, doi:10.1111/febs.16461.
24. Fang, J.; Chai, C.; Qian, Q.; Li, C.; Tang, J.; Sun, L.; Huang, Z.; Guo, X.; Sun, C.; Liu, M.; et al. Mutations of genes in synthesis of the carotenoid precursors of ABA lead to pre-harvest sprouting and photo-oxidation in rice. *Plant J* **2008**, *54*, 177-189, doi:10.1111/j.1365-313X.2008.03411.x.
25. Hwang, S.G.; Lee, C.Y.; Tseng, C.S. Heterologous expression of rice 9-cis-epoxycarotenoid dioxygenase 4 (OsNCED4) in Arabidopsis confers sugar oversensitivity and drought tolerance. *Bot Stud* **2018**, *59*, 2, doi:10.1186/s40529-018-0219-9.
26. Hu, H.; Dai, M.; Yao, J.; Xiao, B.; Li, X.; Zhang, Q.; Xiong, L. Overexpressing a NAM, ATAF, and CUC (NAC) transcription factor enhances drought resistance and salt tolerance in rice. *Proc Natl Acad Sci U S A* **2006**, *103*, 12987-12992, doi:10.1073/pnas.0604882103.
27. Schweighofer, A.; Hirt, H.; Meskiene, I. Plant PP2C phosphatases: emerging functions in stress signaling. *Trends Plant Sci* **2004**, *9*, 236-243, doi:10.1016/j.tplants.2004.03.007.
28. Bhatnagar, N.; Min, M.K.; Choi, E.H.; Kim, N.; Moon, S.J.; Yoon, I.; Kwon, T.; Jung, K.H.; Kim, B.G. The protein phosphatase 2C clade A protein OsPP2C51 positively regulates seed germination by directly inactivating OsbZIP10. *Plant Mol Biol* **2017**, *93*, 389-401, doi:10.1007/s11103-016-0568-2.
29. Yang, Q.; Liu, K.; Niu, X.; Wang, Q.; Wan, Y.; Yang, F.; Li, G.; Wang, Y.; Wang, R. Genome-wide Identification of PP2C Genes and Their Expression Profiling in Response to Drought and Cold Stresses in Medicago truncatula. *Sci Rep* **2018**, *8*, 12841, doi:10.1038/s41598-018-29627-9.

30. Zong, W.; Tang, N.; Yang, J.; Peng, L.; Ma, S.; Xu, Y.; Li, G.; Xiong, L. Feedback Regulation of ABA Signaling and Biosynthesis by a bZIP Transcription Factor Targets Drought-Resistance-Related Genes. *Plant Physiol* **2016**, *171*, 2810-2825, doi:10.1104/pp.16.00469.
31. Hu, Y.; Wu, Q.; Peng, Z.; Sprague, S.A.; Wang, W.; Park, J.; Akhunov, E.; Jagadish, K.S.V.; Nakata, P.A.; Cheng, N.; et al. Silencing of OsGRXS17 in rice improves drought stress tolerance by modulating ROS accumulation and stomatal closure. *Sci Rep* **2017**, *7*, 15950, doi:10.1038/s41598-017-16230-7.
32. Li, D.; Liu, P.; Yu, J.; Wang, L.; Dossa, K.; Zhang, Y.; Zhou, R.; Wei, X.; Zhang, X. Genome-wide analysis of WRKY gene family in the sesame genome and identification of the WRKY genes involved in responses to abiotic stresses. *BMC Plant Biol* **2017**, *17*, 152, doi:10.1186/s12870-017-1099-y.
33. Zhang, X.; Wang, L.; Meng, H.; Wen, H.; Fan, Y.; Zhao, J. Maize ABP9 enhances tolerance to multiple stresses in transgenic Arabidopsis by modulating ABA signaling and cellular levels of reactive oxygen species. *Plant Mol Biol* **2011**, *75*, 365-378, doi:10.1007/s11103-011-9732-x.
34. Kim, M.; Ahn, J.W.; Jin, U.H.; Choi, D.; Paek, K.H.; Pai, H.S. Activation of the programmed cell death pathway by inhibition of proteasome function in plants. *J Biol Chem* **2003**, *278*, 19406-19415, doi:10.1074/jbc.M210539200.
35. Allen, G.C.; Flores-Vergara, M.A.; Krasynanski, S.; Kumar, S.; Thompson, W.F. A modified protocol for rapid DNA isolation from plant tissues using cetyltrimethylammonium bromide. *Nat Protoc* **2006**, *1*, 2320-2325, doi:10.1038/nprot.2006.384.
36. Ning, J.; Li, X.; Hicks, L.M.; Xiong, L. A Raf-like MAPKKK gene DSM1 mediates drought resistance through reactive oxygen species scavenging in rice. *Plant Physiol* **2010**, *152*, 876-890, doi:10.1104/pp.109.149856.
37. Kumar, M.S.S.; Mawlong, I.; Ali, K.; Tyagi, A. Regulation of phytosterol biosynthetic pathway during drought stress in rice. *Plant Physiol Biochem* **2018**, *129*, 11-20, doi:10.1016/j.plaphy.2018.05.019.
38. Du, H.; Wang, N.; Cui, F.; Li, X.; Xiao, J.; Xiong, L. Characterization of the beta-carotene hydroxylase gene DSM2 conferring drought and oxidative stress resistance by increasing xanthophylls and abscisic acid synthesis in rice. *Plant Physiol* **2010**, *154*, 1304-1318, doi:10.1104/pp.110.163741.
39. Qi, J.; Song, C.P.; Wang, B.; Zhou, J.; Kangasjarvi, J.; Zhu, J.K.; Gong, Z. Reactive oxygen species signaling and stomatal movement in plant responses to drought stress and pathogen attack. *J Integr Plant Biol* **2018**, *60*, 805-826, doi:10.1111/jipb.12654.
40. Kalsoom, U.; Bhatti, H.N.; Asgher, M. Characterization of Plant Peroxidases and Their Potential for Degradation of Dyes: a Review. *Appl Biochem Biotechnol* **2015**, *176*, 1529-1550, doi:10.1007/s12010-015-1674-3.
41. Yoshida, T.; Mogami, J.; Yamaguchi-Shinozaki, K. ABA-dependent and ABA-independent signaling in response to osmotic stress in plants. *Curr Opin Plant Biol* **2014**, *21*, 133-139, doi:10.1016/j.pbi.2014.07.009.
42. Takahashi, F.; Kuromori, T.; Sato, H.; Shinozaki, K. Regulatory Gene Networks in Drought Stress Responses and Resistance in Plants. *Adv Exp Med Biol* **2018**, *1081*, 189-214, doi:10.1007/978-981-13-1244-1_11.
43. Hirota, K.; Yoshikiyo, K.; Guilbaud, G.; Tsurimoto, T.; Murai, J.; Tsuda, M.; Phillips, L.G.; Narita, T.; Nishihara, K.; Kobayashi, K.; et al. The POLD3 subunit of DNA polymerase delta can promote translesion synthesis independently of DNA polymerase zeta. *Nucleic Acids Res* **2015**, *43*, 1671-1683, doi:10.1093/nar/gkv023.
44. Palaniyar, N.; Nadesalingam, J.; Clark, H.; Shih, M.J.; Dodds, A.W.; Reid, K.B. Nucleic acid is a novel ligand for innate, immune pattern recognition collectins surfactant proteins A and D and mannose-binding lectin. *J Biol Chem* **2004**, *279*, 32728-32736, doi:10.1074/jbc.M403763200.
45. Zhu, W.; Ma, T.; Zhang, M.; Sha, W. Research progress of receptor-like protein kinases in plants. *Genomics and Applied Biology* **2018**, *37*, 451-458.
46. Allen, T.; Ingles, P.J.; Praekelt, U.; Smith, H.; Whitelam, G.C. Phytochrome-mediated agravitropism in Arabidopsis hypocotyls requires GIL1 and confers a fitness advantage. *Plant J* **2006**, *46*, 641-648, doi:10.1111/j.1365-313X.2006.02727.x.